Journal of Power Sources 203 (2012) 257–261

Contents lists available at SciVerse ScienceDirect

Journal of Power Sources

journal homepage: www.elsevier.com/locate/jpowsour

Short communication

Performance of a graphite (KS-6)/MoO_3 energy storing system

Nanda Gunawardhana[a,*], Gum-Jae Park[a], Arjun Kumar Thapa[a], Nikolay Dimov[a], Manickam Sasidharan[b], Hiroyoshi Nakamura[b], Masaki Yoshio[a,*]

[a] Advanced Research Center, Saga University, 1341 Yoga-machi, Saga 840-0047, Japan
[b] Department of Chemistry and Applied Chemistry, Saga University, 1 Honjo, Saga 840-8502, Japan

ARTICLE INFO

Article history:
Received 27 September 2011
Received in revised form 8 November 2011
Accepted 15 November 2011
Available online 25 November 2011

Keywords:
Safety of batteries
Cathode to anode mass ratio
Cycle performance
Molybdenum oxide anode
Graphite cathode

ABSTRACT

The performance of the graphite (KS-6)/MoO_3 full cell has been studied at different cut-off voltages, rates, temperatures and cathode to anode mass ratios. It was found that cathode to anode weight ratio and charging potential are the most influential parameters which determine the cycle life of this device. Under optimized condition (graphite:MoO_3 weight ratio 1 and operation voltage window 1.5–3.3 V), the capacity retention of the cell between the 5th and 500th cycles was found to be 91%. At 0.3 C and 10 C rates this device delivers 88.9 mAh g^{-1} and 35.5 mAh g^{-1}, respectively. High and low temperature performance of this device is superior to that of the conventional EDLCs. The charge/discharge mechanism of the full cell was elucidated by *ex situ* XRD data and analyzing the voltage profiles of each electrode by 4-electrode cell. Partial amorphization of the MoO_3 anode was confirmed by XRD and SEM data. These results indicate that the electrolyte could be used as the sole source of lithium ions to develop a novel type of energy storage devices which do not contain traditional lithium rich cathode materials.

1. Introduction

Due to high demand of rechargeable energy storage devices, lithium ion batteries (LIBs) and electric double layer capacitors (EDLCs) are being widely used in many applications [1–3]. However, LIBs have insufficient power density and safety [4,5]. On the other hand EDLC, which consists of two activated carbon (AC) electrodes, have a considerably smaller energy density. Nevertheless, the capacitors have attracted worldwide research attention because of their potential application as energy storage devices in many fields. To avoid some of the disadvantages of EDLC, asymmetrical super capacitors were developed. In most of the cases supercapacitor development was achieved by replacing one of the electrodes of the EDLC with a lithium ion battery electrode. In such a super capacitor, the positive electrode stores the charge through a reversible non-Faradaic reaction (absorption), while the negative electrode stores the charge by a reversible Faradaic reaction (intercalation) [7–9].

The same approach allowed us to develop a novel high energy density capacitor called Megalo-capacitance capacitor, in which graphite cathode and activated carbon anode have been used in combination with Li-free electrolytes [10,11]. In this case we have replaced KS-6 graphite for activated carbon positive electrode. Charge storage mechanism at the cathode site consists of absorption and intercalation of anions into the graphite layers. Such a mechanism enables us to increase the capacitance and the working voltage simultaneously. As a result, the energy density of the capacitor is remarkably improved.

Recently, we have developed another electrochemical power source in which metal oxides and graphite are employed as anode and cathode, respectively [10–13]. However, these systems did not show very good cycleability during our preliminary studies because in most of the tests the cathode was charged up to 5.5 V vs. Li/Li^+. At such a high voltage deep intercalation of PF_6^- anions into the graphite cathode takes place, which deteriorates the pristine graphite structure. In addition, uncoated aluminum foil used to make the electrode may enhance the electrolyte decomposition at such a high voltage. To avoid these two effects, we have studied optimal cathodic potentials and used carbon coated aluminum foil as a current collector.

In this work we describe the features of our novel capacitor composed of graphite cathode and MoO_3 anode. The performance of this energy storage system was tested at different cut-off voltages and different temperatures to examine its performance. To understand the overall reaction mechanism, the voltage profiles were obtained by 4-electrode cell which is recording simultaneously the potential profiles of the half-cells Li/MoO_3 and Li/graphite. *Ex situ* XRD data were collected at fully charged and discharged states to get more insight of the structural changes of the electrodes. SEM images were used to analyze the morphological changes of the MoO_3 electrode after cycling.

* Corresponding authors. Tel.: +81 952 20 4729; fax: +81 952 20 4729.
E-mail addresses: kgngu@yahoo.com (N. Gunawardhana), yoshio@cc.saga-u.ac.jp (M. Yoshio).

0378-7753/$ – see front matter © 2011 Elsevier B.V. All rights reserved.
doi:10.1016/j.jpowsour.2011.11.048

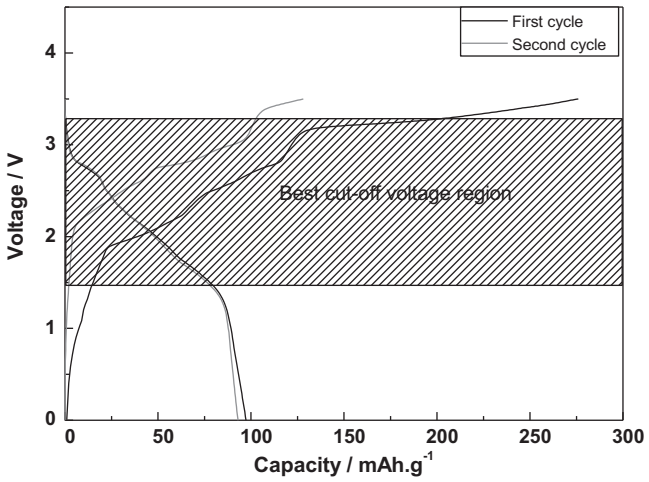

Fig. 1. The initial charge/discharge curves for Li/1 M $LiPF_6$-EC/DMC (1:2)/MoO_3 with a current density of 100 mA g^{-1} between 0.0 and 3.5 V at room temperature.

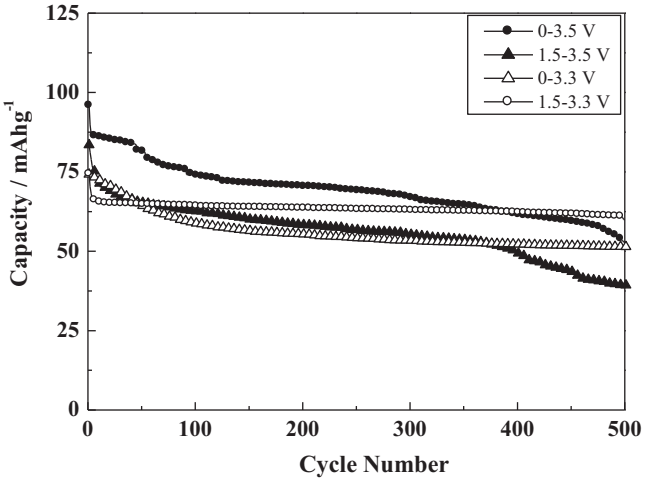

Fig. 2. Cycleability of KS-6/MoO_3 cell with different cut-off voltages.

2. Experimental

Artificial graphite KS-6 (Timcal Co. Ltd., Switzerland) was used as a cathode material and commercial MoO_3 (Wako Co. Ltd., Japan) was used as an anode material. The slurry was cast into carbon coated aluminum foil current collector. The electrodes were first dried at 120 °C then punched out into disks having 2 cm^2 cross sectional area. The electrochemical characterizations were performed using a CR2032 coin-type cells. The electrodes were pressed under 300 kg cm^{-2} and vacuum dried at 160 °C for 4 h. The positive and negative electrodes were separated by two glass fiber filters and the amount of the electrolyte was ca. 0.5 mL. The electrolyte was 1.0 M $LiPF_6$-EC:DMC (1:2 by volume) supplied by Ube Chemicals Co. Ltd., Japan. Mass loading of electrodes was 4–6 mg cm^{-2}. The cycle life test was carried out at a current density of 100 mA g^{-1}. Powder X-ray diffraction (XRD, MINIFlex II, Rigaku, Japan) using CuKα radiation was employed to identify the intercalation of the PF_6^- anions and structural changes in positive and negative electrodes under various states of charges. In such a test the coin cells were disassembled at a desired state of charge and both graphite and MoO_3 electrodes were recovered in an argon filled glove box. After being washed with DMC, the electrodes were sealed in polyvinyl bags to prevent any reaction with the air and their XRD patterns were immediately recorded. Other experimental details and instrumentation methods are described elsewhere [11,13].

3. Results and discussion

Fig. 1 shows the first and second charge/discharge curves of the KS-6/1 M $LiPF_6$-EC/DMC (vol. 1:2)/MoO_3 energy storage system in the voltage window 0–3.5 V. We performed several primary tests in the voltage ranges of 0–3.5 V, 0–3.3 V and 1.5–3.3 V, to select best cut-off voltage range for this capacitor.

During the first charge this capacitor shows initial sudden voltage increase up to 2.2 V but the capacity at this stage is small as the amount of the anions adsorbed to the edge plane regions of the graphite is not large. This is because the surface area of graphite is much smaller than that of AC. When the voltage increases further PF_6^- anions start to intercalate within the graphite layers. It is notable that the later process has a major contribution to the overall capacity of the cathode. This indicates that energy storage process in this hybrid capacitor has gradually changed from electric double layer electrostatic absorption to Faradaic type of electrochemical reaction. When the charging voltage is 3.3 V the initial charging capacity is 242 mAh g^{-1}. However, with the increase of the voltage up to 3.5 V, the initial charging capacity increases to 326 mAh g^{-1}. The full discharge capacities of these stages are 88 and 97 mAh g^{-1} respectively. From these results it can clearly be seen that first cycles have significantly higher irreversible capacity. This irreversible capacity could be attributed to two main factors:

1. Partial amorphization of MoO_3 anode accompanied by partial electrolyte decomposition.
2. The irreversible capacity coming from anion intercalation into the graphite and its partial exfoliation.

When the charging potential increases this irreversible capacity becomes much larger due to enhanced anion intercalation and electrolyte decomposition on the surface of graphite operating at higher voltages. During the second cycle the charge and discharge capacities of the cell in the voltage region 0–3.3 V are 103 and 83 mAh g^{-1}. When the charging potential rises up to 3.5 V these two values became 128 and 90 mAh g^{-1}, respectively. Fig. 2 shows the variation of discharge capacities of KS-6/MoO_3 system within various cut-off voltage windows. When the cut-off voltage is 0–3.5 V capacity retention of between 5th and 500th cycle is about 62%.

Therefore full charging of these cells induces significant capacity fading. However analysis of the fully charged electrodes by 4 electrode cell let us determine the ceiling potential of KS-6 and optimize its cycle life. Voltage profile recorded by 4 electrode cells revealed that 3.5 V cut-off voltage of the MoO_3/KS-6 full cell corresponds to 5.5 V KS-6 vs. Li/Li^+. Such a high voltage boosts the energy density but leads to a deeper PF_6^- intercalation which causes large volume expansion of the pristine KS-6 crystal structure. This effect might cause severe structural transformations and deteriorate the capacitor during prolonged cycling. We have tested this hypothesis by gradual narrowing of the voltage window. Decreasing the upper cut-off voltage from 3.5 V down to 3.3 V (5.3 V KS-6 vs. Li/Li^+) improves capacity retention between the 5th and the 500th cycle from 62 to 70%. Further decrease of the upper cut-off voltage would decrease the energy density of this system. On the other hand increasing the lower cut-off voltage almost does not decrease the energy density of this system because the discharge curve between 1.5 and 0.0 V is almost vertical. Increasing the lower cut-off voltage from 0.0 to 1.5 V further boosts the capacity retention to 91% between the 5th and 500th cycles. Therefore the best cut-off voltage window of the MoO_3/KS-6 energy storage device is 1.5–3.3 V shown as a shaded rectangle in Fig. 1.

Fig. 3 exhibits the rate capabilities of KS-6/MoO_3 with mass ratio of 1:1 in the voltage range of 1.5–3.3 V. At 0.3 C rate it delivers

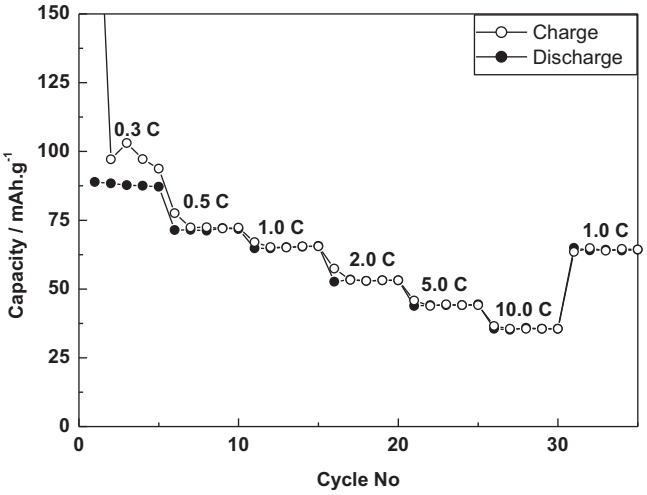

Fig. 3. The rate performance of KS-6/MoO_3 capacitor in the voltage range of 1.5–3.3 V.

88.9 mAh g^{-1}. As shown in Fig. 3, when the charge/discharge rate increases, the specific capacities decrease gradually. At 10 C rate its discharge capacity is 35.5 mAh g^{-1}. Fig. 4 shows the temperature dependence of the KS-6/MoO_3. At 60 °C it shows higher discharge capacity due to higher mobility of lithium and PF_6^- anions. At that temperature initial discharge capacity was 86 mAh g^{-1}. After 10 cycles, the capacity retention was 92%. As shown in Fig. 3, when temperature decreases to 0 °C, the discharge capacity drops drastically in the initial 10–15 cycles. Then the discharge capacity retains about 30 mAh g^{-1}. However, even at such a low temperature the energy density of KS-6/MoO_3 is still higher than EDLCs owing to the higher charging voltage and larger capacity of the working electrodes.

From our previous data, we have noted that the capacity of the MoO_3/Li half cell is about 197 mAh g^{-1} for the first discharge process in the voltage region of 1.0–3.0 V vs. Li/Li^+. To extract the maximum capacity from MoO_3 anode in the KS-6/MoO_3 full cell, we then changed the weight ratio of MoO_3 and KS-6 electrodes. To analyze the effect of the mass balance between the electrodes we have charged/discharged the full cell in the voltage region of 1.5–3.3 V. The cycling behavior of the full cells with different KS-6 to MoO_3 mass ratios is shown in Fig. 5. It is clear that higher KS-6/MO_3 weight ratios yield higher capacity delivered from the anode. However, the capacity retention of the cell gradually decreases with

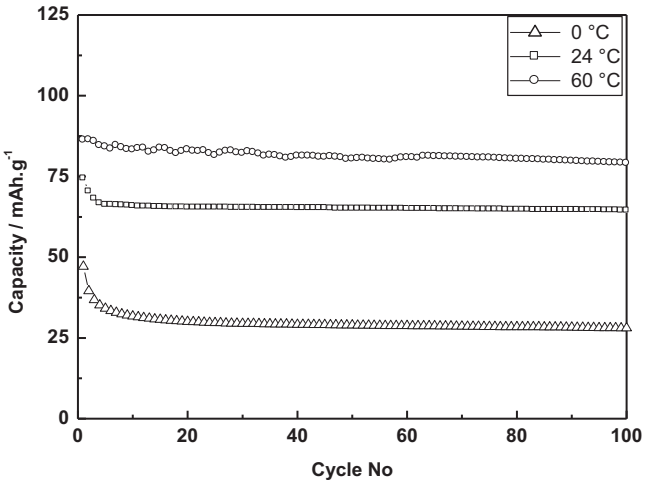

Fig. 4. The cycleability of KS-6/MoO_3 capacitor at various temperatures in the voltage region of 1.5–3.3 V.

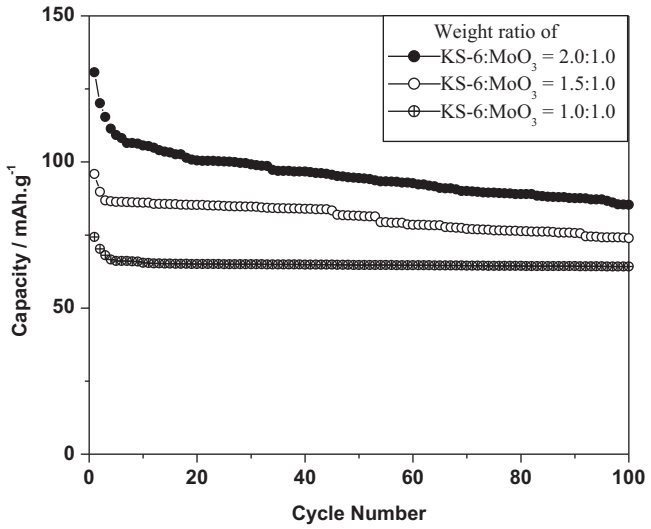

Fig. 5. The effects of mass balance of KS-6:MoO_3 for the capacity and cycleability of cell.

increasing weight ratio of KS-6/MoO_3. When the KS-6/MoO_3 ratio is 2:1, the first discharge capacity of the full cell is 130.7 mAh g^{-1} but the capacity retention from the 5th to the 100th cycle becomes 75.8%. By decreasing the weight ratio of KS-6/MoO_3 from 1.5 to 1, capacity retention of the full cell between the 5th and the 100th cycle increased up to 85.7%. When we further decrease the mass ratio down to 1:1, the capacity retention of the cell between the 5th and the 100th cycles increased up to 96.3%. Therefore the best mass ratio of KS-6:MoO_3 allowing prolonged cycling is 1:1.

The ceiling voltage and bottom voltage of KS-6/MoO_3 system with increasing the weight ratio of the cathode to the anode from 1:1 to 2:1 is shown in Fig. 6. The ceiling voltages of KS-6 electrode decreased from 5.35 to 5.02 V by increasing the weight ratio in KS-6/MoO_3 system. On the other hand the bottom voltages of MoO_3 anodes have decreased simultaneously from 2.05 to 1.72 V maintaining the overall charging potential 3.3 V. Fig. 6 also shows that beyond the point MoO_3:KS-6 = 1.5 both the ceiling voltage of KS-6 and the bottom voltage of MoO_3 decrease faster and the cycle life of the cell worsens.

Therefore the cycle performance of KS-6:MoO_3 full cells could further be improved by changing the cut-off voltages at each

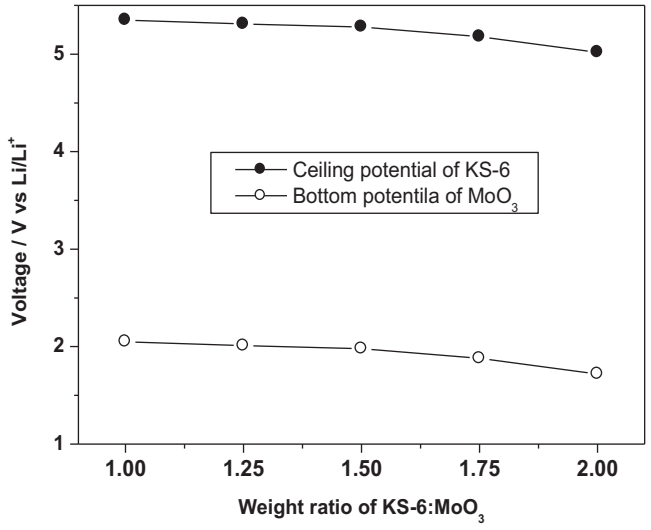

Fig. 6. The variation of the ceiling voltage and bottom voltage of KS-6 and MoO_3 electrodes in different mass ratio of KS-6:MoO_3.

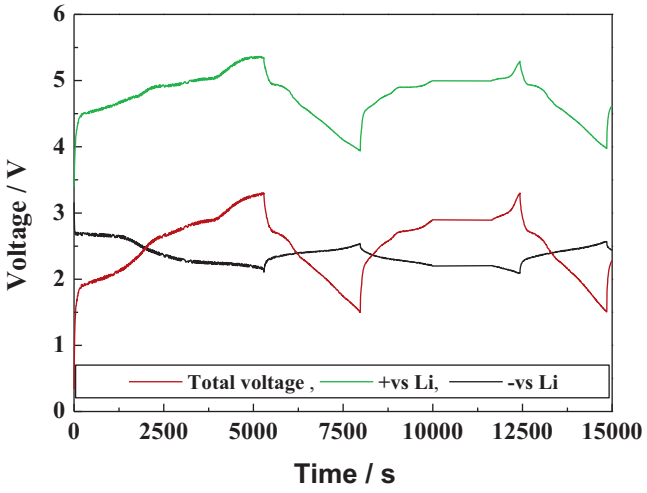

Fig. 7. Potential profiles of KS-6/MoO_3 cell during the galvanostatic charge/discharge process. The positive and negative electrodes have the same weight of active material.

cathode/anode weight ratio. However, at this point we are optimizing the cut-off voltages of the full cells with respect to each mass ratio. By adjusting the cut-off voltages, we believe that the performance of the cell could be further improved because energy density, swing voltage, and specific capacitance are all functions of the electrode mass ratio and ion concentration of the electrolyte.

Fig. 7 shows the potential profiles of the KS-6 positive and MoO_3 negative electrodes with respect to two Li metal reference electrodes in a 1.0 M $LiPF_6$ (EC/DMC = 1/2 (v/v)) solution. In the initial charge process, the potential of the MoO_3 negative electrode initially drops down to 2.7 V against Li metal. MoO_3 shows voltage plateaus around 2.7 and 2.4 V at the first charge. There is a gradual voltage decrease between 2.7 and 2.2 V from the second cycle. Structural change in the crystal lattice of MoO_3 is anticipated during charge/discharge in this voltage range. On the other hand, during the first charging, the voltage of KS-6 electrode jumps suddenly to 4.5 V against Li metal. At this stage PF_6^- anions absorb to edges and surfaces of KS-6 electrode. When PF_6^- anions start inserting into the interlayer spaces of KS-6, this sudden potential rise becomes a sloppy curve, indicative of an intercalation. This results in a bent shape of the voltage profile, which gradually increases until it reaches to the ceiling potential of cathode. During the discharge process, the potential of MoO_3 gradually increases from 2.2 to 2.5 V vs. Li/Li^+ while the potential of KS-6 first drops down to 5.0 V then gradually decreases to 4.0 V. These two processes maintain the voltage of this device between 1.5 and 3.3 V. Moreover, the first discharge time is significantly shorter than charging time. This is because of the electrolyte decomposition in the first charging process. However, the charge/discharge times of the second cycle do not show significant difference.

In order to investigate the reaction mechanism and structural changes of the cathode and the anode, *ex situ* XRD experiments were conducted. Fig. 8(a) shows *ex situ* XRD diffractions of the KS-6 electrode in the KS-6/MoO_3 energy storage system, before, after first charge (3.3 V) and after first discharge (1.5 V) processes. In well ordered KS-6 the (0 0 2) peak at 26.5° could be used as an indicator for structural changes of the KS-6 cathode. When this cell is charged to 3.3 V (5.3 V vs. Li/Li^+) the (0 0 2) peak shifts to 24.3° due to anion intercalation into graphite. This observation is in good agreement with the literature [14–19]. During discharge, the peak position of the 0 0 2 peak does not fully come back to its original position. Instead, a broader peak appeared centering at 25.9° in XRD. This indicates partial structural changes of graphite during

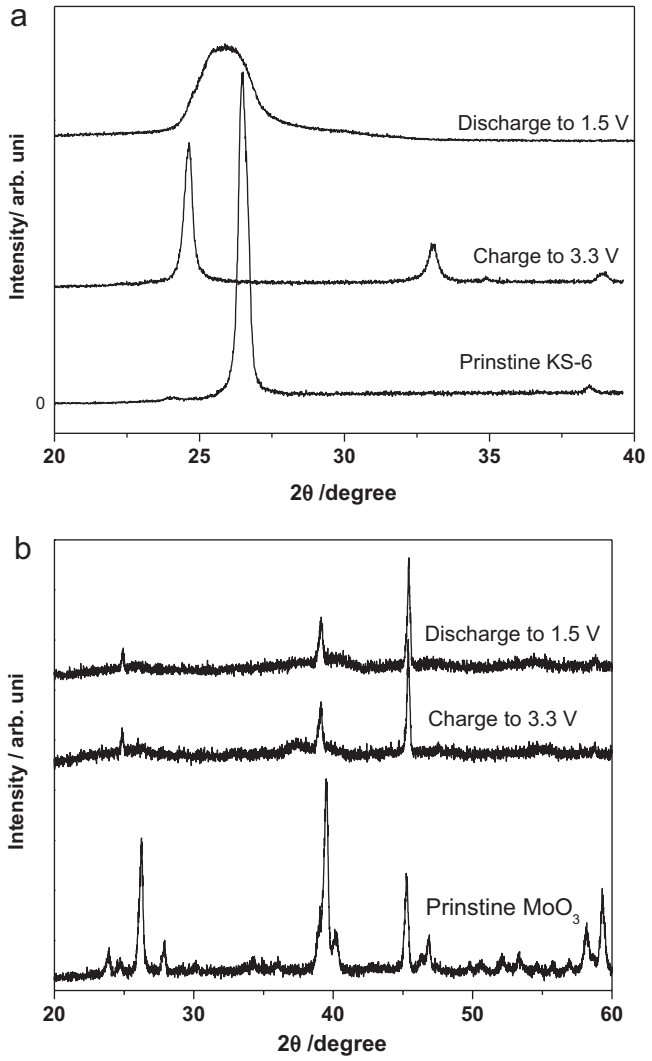

Fig. 8. *Ex situ* XRD patterns of the (a) KS-6 and the (b) MoO_3 electrodes, after the first charge and discharge processes.

cycling. In addition, the peak intensity of the electrode in its discharged state is relatively low compared to that of the pristine KS-6. These observations are in agreement with Seel and Dahn data [18].

Fig. 8(b) shows the *ex situ* XRD patterns of MoO_3 anode in its pristine state after first charge (3.3 V) and after first discharge (1.5 V). MoO_3 used in this study has an orthorhombic structure with lattice parameters of $a = 6.05$ Å, $b = 29.04$ Å, and $c = 3.86$ Å. Unlike graphite, after charging up to 3.3 V (2.0 V vs. Li/Li^+) the original peak position of MoO_3 disappeared. This could be attributed to the structural changes of MoO_3 from orthorhombic to partially amorphous state [16,20,21]. This was confirmed by discharging the full cell back to zero volts. During the discharging some of the original peaks of MoO_3 such as (1 1 0), (0 0 4), (0 2 1), and (0 6 0) did not re-appear in the XRD pattern which indicates its partial amorphization. During the initial reduction, a part of the intercalated lithium is irreversibly trapped in the oxide to form $Li_{x+y}MoO_3$. During the de-insertion and subsequent cycles, only x moles of lithium could be reversibly inserted and de-inserted. These two processes could be summarized as follows.

$$(x+y)Li^+ + (x+y)e^- + MoO_3 \xrightarrow[\text{Conversion}]{\text{First cycle}} Li_{x+y}MoO_3$$

$$xLi^+ + xe^- + Li_yMoO_3 \xrightarrow{\text{Cycling}} Li_{x+y}MoO_3$$

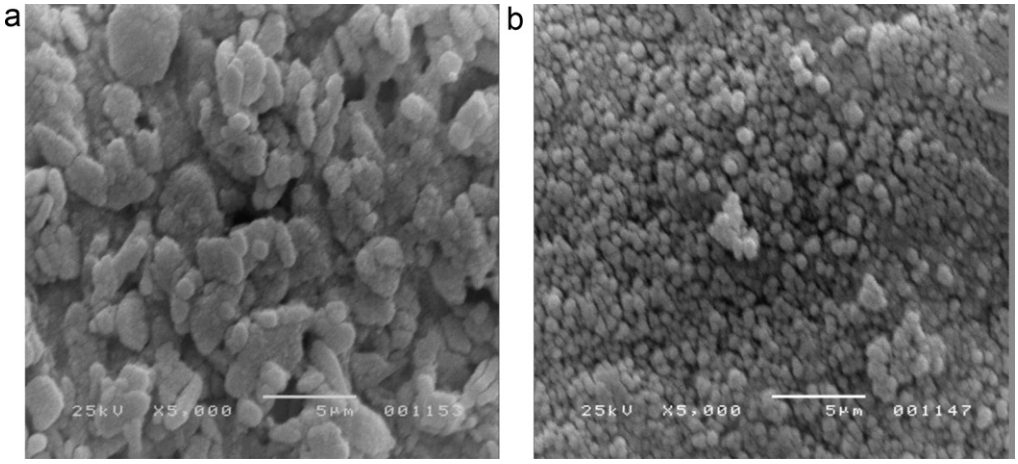

Fig. 9. SEM images of MoO_3 anode (a) before and (b) after first cycle.

Therefore complete lithium extraction is not possible during the first discharging. This result is in agreement with a previous study showing that the kinetically accessible stoichiometric range of the reversible lithium insertion/de-insertion is $0.1 < y < 1.5$ in Li_zMoO3 ($z = x + y$) [6,21]. Though the potential of the full cell is increased up to 3.3 V, confirmed with the 4-electrode cell, the voltage of MoO_3 anode only changes from 2.6 to 2.0 V vs. Li/Li^+. As a result, MoO_3 is cycled in a quasi-amorphous state in the range of 0–3.3 V. Despite this partial amorphization, MoO_3 is the most stable metal oxide so far tested with KS-6 cathode [12,13,22]. Partial amorphization is further confirmed by SEM images of MoO_3 electrode. Fig. 9 compares the electrode morphologies of MoO_3 before and after the first cycle. The figure clearly shows that during the first cycle the larger particles break down into smaller ones. This is clear evidence for partial amorphization, which is in agreement with XRD data.

The *ex situ* XRD, SEM, and electrochemical results could be used to elucidate the intercalation mechanism of $LiPF_6$ into graphite cathode and MoO_3 anode. Upon charging of the KS-6/MoO_3 full cell, Li^+ and PF_6^- ions in the electrolyte solution migrate towards their respective electrodes. The PF_6^- ions intercalate into the interlayer spaces of the graphite cathode electrode, while the Li^+ ions get into the MoO_3 anode and transform it into partially amorphous state. The first step of the charging process takes place in the voltage region from 0 to 2.2 V and involves adsorption of PF_6^- to the edge-plane surfaces of graphite. The second step of the charging reaction proceeds when potential exceeds 2.0 V and involves PF_6^- intercalation into KS-6 and Li^+ insertion into MoO_3. When the KS-6/MoO_3 cell is discharged, the Li^+ and PF_6^- ions are extracted from their respective electrode structures and reconstitute the original $LiPF_6$ electrolyte solution. This type of electrochemical device does not fall into any of the existing categories, i.e. they are neither capacitors nor rechargeable batteries.

4. Conclusions

In this work we studied in detail new energy storage system, which consists of KS-6 cathode and MoO_3 anode. It is clearly demonstrated that cathode to anode weight ratio and charging potential are the most influential parameters which determine the cycle life of device. KS-6:MoO_3 weight ratio 1 and operation voltage window 1.5–3.3 V were found as optimum values allowing cycle life comparable to that of modern lithium ion batteries. The possibility of long cycle life of graphitic cathodes undergoing deeper PF_6^- intercalation paves the way for development of electrochemical energy storage devices with transition metal free cathodes. Data also show that the electrolyte could be used as the sole source of lithium ions. The KS-6 cathode can be charged to the highest voltages without the threat of oxygen release and explosions like reactions. On the other hand metal oxides have a higher intercalation voltage which precludes lithium deposition. Therefore, this kind of electrochemical devices are inherently safer than lithium ion batteries and possess higher energy density than EDLC.

Acknowledgment

Partial financial support from Fukuoka Industrial Science Foundation is gratefully acknowledged.

References

[1] P.G. Bruce, B. Scrosati, J.M. Tarascon, Angew. Chem. Int. Ed. 47 (2008) 2930–2946.
[2] D.H. Jurcakova, M. Seredych, Y. Jin, G.Q. Lu, T.J. Bandosz, Carbon 48 (2010) 1767.
[3] P. Sharma, T.S. Bhatti, Energy Conversion and Management 51 (2010) 2901–2912.
[4] W. Fergus, J. Power Sources 195 (2010) 939.
[5] N. Gunawardhana, N. Dimov, G.-J. Park, M. Sasidharan, H. Nakamura, M. Yoshio, Electrochem. Commun. 13 (2011) 1116.
[6] H. Arai, M. Tsuda, K. Saito, M. Hayashi, Y. Sakurai, J. Electrochem. Soc. 149 (2002) A401.
[7] B.E. Conway, Electrochemical Supercapacitor – Scientific Fundamentals and Technological Application, Kluwer Academic, New York, 1999, pp. 29–31.
[8] A. Burke, J. Power Sources 91 (2000) 37.
[9] O. Barbieri, M. Hahn, A. Herzog, R. Kotz, Carbon 43 (2005) 1303.
[10] M. Yoshio, H. Nakamura, H. Wang, Electrochem. Solid State Lett. 9 (2006) A561.
[11] H. Wang, M. Yoshio, Electrochem. Commun. 8 (2006) 1481.
[12] A.K. Thapa, G. Park, H. Nakamura, T. Ishihara, N. Moriyama, T. Kawamura, H. Wang, M. Yoshio, Electrochim. Acta 55 (2010) 7305.
[13] N. Gunawardhana, G.-J. Park, N. Dimov, A.K. Thapa, H. Nakamura, H. Wang, T. Ishihara, M. Yoshio, J. Power Sources 1 (2011) 119.
[14] N. Koshiba, K. Takata, M. Nakanishi, Z. Takehara, Denki Kaguku 62 (1994) 631.
[15] D. Aurbach, H. Teller, M. Koltypin, E. Levi, J. Power Sources 1 (2003) 119.
[16] M. Holzapfel, H. Buqa, F. Krumeich, P. Novak, F.M. Petrat, C. Veit, Electrochem. Solid State Lett. 8 (2005) A516.
[17] N. Bartlet, B.W. Mcquillan, in: M.S. Whittingham, A.J. Jacobson (Eds.), Intercalation Chemistry, Academic Press, New York, 1982, pp. 19–50.
[18] J.A. Seel, J.R. Dhan, J. Electrochem. Soc. 147 (2000) 892.
[19] P.W. Ruch, M. Hahn, F. Rosciano, M. Holzapfel, H. Kaiser, W. Scheifele, B. Schmitt, P. Novak, R. Kotz, A. Wokaun, Electrochim. Acta 53 (2007) 1074.
[20] J.O. Besenhard, J. Heydecke, H.P. Fritz, Solid State Ionics 6 (1982) 215.
[21] Y. Iriyama, T. Abe, M. Inaba, Z. Ogumi, Solid State Ionics 135 (2000) 95–100.
[22] G.J. Park, D. Kalpana, A.K. Thapa, H. Nakamura, Y.S. Lee, M. Yoshio, Bull. Korean Chem. Soc. 30 (4) (2009) 817.